



Seismic Stability Analysis of Soil Nail Walls Using the Upper Bound Method

Meysam Imani¹ · Omid Babaei Pouya¹

Accepted: 9 November 2020 / Published online: 7 January 2021
© Springer Science+Business Media, LLC, part of Springer Nature 2021

Abstract

Soil nailing can be considered one of the most useful methods for ensuring the stability of excavations. The static stability analysis of the soil nail walls is necessary for practical applications. Moreover, for the walls that are intended to be used in a long time, seismic stability analysis is also required, which is the main subject of the present paper. The upper bound method of limit analysis was used to develop the formulation of the safety factor of the soil nail walls. The effect of both the horizontal and vertical accelerations of the earthquake was considered in the calculations. It was assumed that the wall is not inclined with respect to the vertical direction. Also, the method presented in this paper is capable of considering the effects of both the surcharge loads and different inclinations of the ground above the wall. The obtained results show that the horizontal and vertical accelerations of the earthquake result in decreasing the safety factor of soil nail walls. Also, the safety factor of the stability of the soil nail walls is affected by different parameters, including the soil and nail properties and the geometrical configuration of the problem. Extensive sensitivity analyses were performed to investigate the effect of all important parameters on the safety factor.

Keywords Excavation · Soil nailing · Upper bound method · Stability analysis · Safety factor

1 Introduction

In recent years, demand in large structures which have several basement floors was increased. Generally, such structures require deep excavations, which their stabilization is a challenging issue in geotechnical engineering problems. One of the most common methods for stabilizing such excavations is soil nailing. High construction speed,

✉ Meysam Imani
imani@aut.ac.ir

¹ Geotechnical Engineering Group, Amirkabir University of Technology, Garmsar Campus, Garmsar, Iran

simultaneous excavation phases, easy access to drilling machines, and appropriate costs are the main reasons for the popularity of this method. In this method, it is necessary to obtain an optimal pattern of the nails, which requires an overall system stability analysis.

Most available methods for the analysis of the soil nail walls are based on the limit equilibrium method. In the framework of this method, Mittal (Mittal 2006) proposed that increasing the internal friction angle and cohesion of the soil results in improving the stability of the soil nail walls. Also, Meenal et al. (Meenal et al. 2009) proposed a method for quasi-static analysis of oblique nail walls.

Using the limit equilibrium method for stability analysis of geotechnical structures may lead to misleading results since it is unclear whether the obtained results correspond precisely to the failure state or are slightly different (smaller or larger) from the exact failure load. This limitation will be eliminated by using the limit analysis method. The safety factor obtained by using this method is the upper/lower bound of the exact safety factor. There exist some essential studies based on this method in the literature (Meenal et al. 2009; Chen and Liu 1990; Michalowski 1998; Giri and Sengupta 2009; He et al. 2012; Yang et al. 2020).

The experimental method was also used by researchers for analyzing soil nail walls. Zhou et al. (Zhou et al. 2009) conducted some actual scale tests for investigating the stability of soil nail walls. Moradi et al. (Moradi et al. 2020) performed four centrifuge tests to investigate the effect of convex corners on the deformation of soil-nailed walls. They evaluated the wall behavior according to the layout of nails. Also, the results of several pullout tests were used by Sharma et al. (Sharma et al. 2020) to investigate the behavior of helical nails in dry cohesionless soils under static and seismic conditions. They proposed a pullout capacity equation which can be used for stability analysis of helical soil-nailed walls. Jaya and Joy (Jaya and Joy 2013) and Rawat et al. (Rawat et al. 2013) used both laboratory tests and numerical methods for determining the safety factor of soil nail walls. In addition to the mentioned method, the application of numerical methods for stability analysis of soil nail walls becomes very common in recent years. Some of the essential works on this basis can be found in the literature (Giri and Sengupta 2010; Zhou and Yin 2008; Clarke et al. 2013; Babu et al. 2007).

Due to the difficulties in preparing laboratory models of soil nail walls, as well as the high sensitivity of the numerical methods to the input parameters, analytical methods generally provide a simple framework for determining the safety factor of soil nail walls. The importance and simplicity of such methods are crucial in the early stages of engineering project studies.

In the present paper, using the upper bound method of limit analysis, an equation for the safety factor of soil nail walls was developed, which can be used in both static and seismic conditions. The Mohr–Coulomb failure criterion was used for the soil, and the effects of the surcharge and inclined ground surface at the top of the wall were incorporated into the upper bound formulation.

2 The Basics of the Upper Bound Method of Limit Analysis

Dealing with the stability problems requires solving the stress equilibrium equations along with satisfying the compatibility conditions, simultaneously, which is too difficult even in simple problems. In the upper bound method, this procedure can be performed more simply by ignoring the stress equilibrium conditions. According to

the upper bound method, in a kinematically admissible failure mechanism, the load obtained by equating the external work and the internal dissipated energy is not less than the actual failure load. Therefore:

$$\int_V \sigma_{ij} \dot{\varepsilon}_{ij} dV \geq \int_S T_i v_i ds + \int_V X_i v_i dV \quad (1)$$

where σ_{ij} and $\dot{\varepsilon}_{ij}$ are the stress and strain tensors in any admissible velocity field, T_i is any surface traction applied to the failure mechanism, s is the admissible velocity field, X_i is the body force, V is the volume of the failure mechanism, and v_i is the velocity along each discontinuity line. The upper bound limit analysis involves the solution of Eq. 1, which results in finding the optimal solution among the numerous acceptable answers.

3 Determination of the Safety Factor Using the Upper Bound Method

3.1 Selection of the Failure Mechanism

Two types of failure mechanisms were commonly used in the stability analysis of excavations, which include the multi-wedge translational failure mechanism and the rotational failure mechanism. The existing researches show that the rotational failure mechanism results in a more accurate safety factor (Zhou et al. 2009; Jaya and Joy 2013; Rawat et al. 2013; Giri and Sengupta 2010; Zhou and Yin 2008; Clarke et al. 2013; Babu et al. 2007). Therefore, it was used in this paper for obtaining the equation of the safety factor for soil nail walls subjected to static and seismic loadings, as shown in Fig. 1. This mechanism is capable of considering the inclination of the ground surface. Assuming that the failure surface is perpendicular to the ground surface, it can be proved that θ_0 is equal to ϕ (Giri and Sengupta 2009).

The equation of the logarithmic spiral failure line is as follows:

$$r_h = r_0 e^{(\theta_h - \theta_0) \tan \phi} \quad (2)$$

where r_0 and r_θ are the radiuses corresponding to the angles θ_0 and θ_h , respectively, and ϕ is the soil internal friction angle. Based on the geometrical relations, the value of r_0 can be obtained as follows (Mittal 2006):

$$r_0 = \frac{H \sin \lambda \cot \beta - H \cos \lambda}{e^{(\theta_i - \theta_0) \tan \phi} \cos \lambda \sin \theta_h + e^{(\theta_h - \theta_0) \tan \phi} \sin \lambda \cos \theta_h - \sin \theta_0 \cos \lambda \cos \theta_0} \quad (3)$$

3.2 Calculation of the External Work

3.2.1 The External Work Due to the Weight of the Soil Mass

Based on Fig. 2, the general form of the external work performed by the weight of the moving soil mass, i.e., part abc , can be obtained as follows:

$$W = M\omega \quad (4)$$

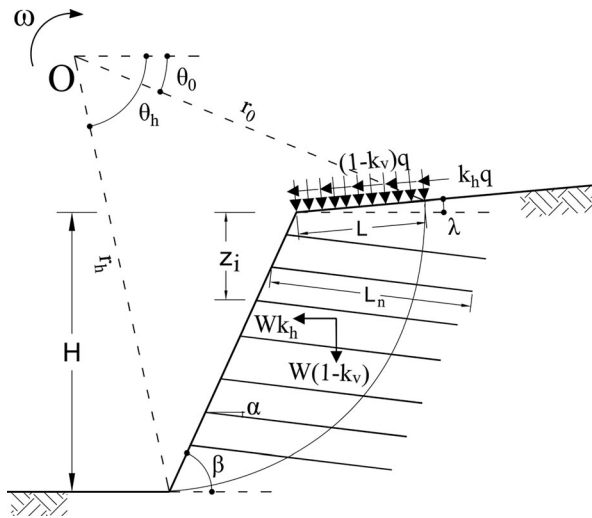


Fig. 1 The rotational failure mechanism considered in this study

where M is the moment due to the weight of the moving soil mass, and ω is the angular velocity. It is difficult to calculate the external work performed by the weight of the abc part directly. Therefore, it was calculated by using the principle of superposition as follows:

$$W_{abc} = W_{oab} - W_{ocb} - W_{oca} \tag{5}$$

where W_{abc} , W_{oab} , W_{ocb} , and W_{oca} are the external works performed by the weight of the parts abc , oab , ocb , and oca , respectively.

Also, the effect of the earthquake on the soil mass was considered horizontal and vertical body forces applied to the center of gravity of the moving soil mass, which are equal to $F_v = k_v W$ and $F_h = k_h W$, respectively. k_v and k_h are the earthquake vertical and horizontal accelerations, respectively, and W is the weight of the moving soil mass

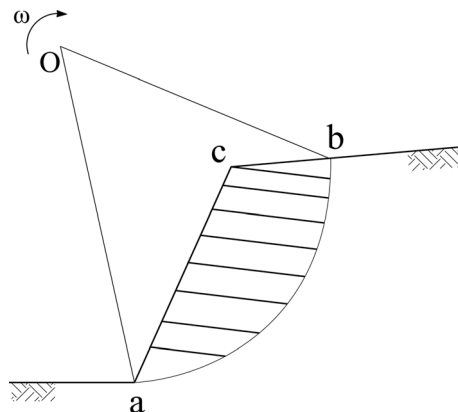


Fig. 2 The moving soil mass

($W = W_{abc}$). Therefore, the general forms of the vertical and horizontal external works due to the soil mass are as follows, respectively:

$$W_v = (1 - k_v) \omega \gamma r_0^3 (f_1 - f_2 - f_3) \quad (6)$$

$$W_h = k_h \omega \gamma r_0^3 (f_4 - f_5 - f_6) \quad (7)$$

where the factors f_1 to f_6 are as follows:

$$f_1 = \frac{(3 \tan \phi \cos \theta_h + \sin \theta_h) e^{3(\theta_h - \theta_0) \tan \phi} - 2 \sin \theta_0}{3(1 + 9 \tan^2 \phi)} \quad (8)$$

$$f_2 = \frac{1}{6} \cdot \frac{L}{r_0} \left(2 \cos \theta_0 - \frac{L}{r_0} \cos \lambda \right) \sin(\theta_0 + \lambda) \quad (9)$$

$$f_3 = \frac{1}{6} e^{(\theta_h - \theta_0) \tan \phi} \left[\sin(\theta_h - \theta_0) - \frac{L}{r_0} \sin(\theta_h + \lambda) \right] \cdot \left[\cos \theta_0 - \frac{L}{r_0} \cos \lambda + \cos(\theta_h + \lambda) e^{(\theta_h - \theta_0) \tan \phi} \right] \quad (10)$$

$$f_4 = \frac{(3 \tan \phi \sin \theta_h - \cos \theta_h) e^{3(\theta_h - \theta_0) \tan \phi} - 3 \tan \phi \sin \theta_0 + \cos \theta_0}{3(1 + 9 \tan^2 \phi)} \quad (11)$$

$$f_5 = \frac{1}{3} \cdot \frac{L}{r_0} \sin^2(\theta_0 + \lambda) \quad (12)$$

$$f_6 = \frac{1}{6} e^{(\theta_h - \theta_0) \tan \phi} \left[\sin(\theta_h - \theta_0) - \frac{L}{r_0} \sin(\theta_h + \lambda) \right] \cdot \left[\sin \theta_0 + e^{(\theta_h - \theta_0) \tan \phi} \sin \theta_h \right] \quad (13)$$

in which L is shown in Fig. 1, and its value can be obtained as follows:

$$\frac{L}{r_0} = \frac{\sin(\theta_h - \theta_0)}{\sin \theta_h} - \frac{\sin(\theta_h + \beta)}{\sin \theta_h \sin \beta} \left[e^{(\theta_h - \theta_0) \tan \phi} \sin \theta_h - \sin \theta_0 \right] \quad (14)$$

3.2.2 The External Work Due to the Surcharge

As shown in Fig. 1, the surcharge q was applied to a length equal to L to the top of the wall. The external work due to the surcharge comprises the work due to itself and the work due to the effect of the earthquake on it. Therefore, the total vertical and horizontal works due to the surcharge are as follows, respectively:

$$W_{qv} = \omega q L \cos \lambda (1 - k_v) \left(r_0 \cos \theta_0 - \frac{L}{2} \cos \lambda \right) \quad (15)$$

$$W_{qh} = \omega qL \sin \lambda k_h \left(r_0 \cos \theta_0 - \frac{L}{2} \cos \lambda \right) \tag{16}$$

3.2.3 The Total External Work

Summing the external works performed by different forces, the total external work in the whole mechanism can be calculated as follows:

$$W = W_v + W_h + W_{qv} + W_{qh} \tag{17}$$

3.3 Calculation of the Internal Energy Dissipation

3.3.1 The Energy Dissipation Due to the Soil Cohesion

Part of the energy dissipation in the failure mechanism is due to the soil cohesion which occurred along the velocity discontinuity lines and can be calculated as the summation of the multiplication of the soil cohesion by each discontinuity line length and by the velocity component along the discontinuity line. Therefore, the total energy dissipation along all velocity discontinuity lines is equal to:

$$D_c = \int_{\theta_0}^{\theta_h} cr \omega \cos \phi \frac{rd\theta}{\cos \phi} = \frac{cr_0^2 \omega}{2 \tan \phi} \left[e^{2(\theta_h - \theta_0) \tan \phi} - 1 \right] \tag{18}$$

3.3.2 The Energy Dissipation Due to the Nails

The moment produced by the nail forces about the center of rotation of the failure surface, i.e., point *O* in Fig. 1, induces an energy dissipation that should be added to the total energy dissipation along the velocity discontinuity lines. According to Fig. 3,

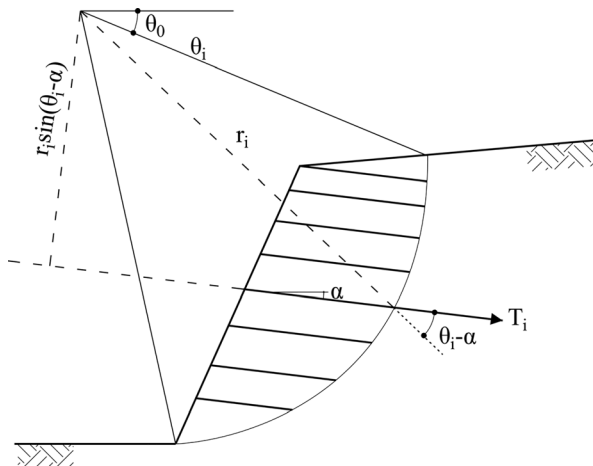


Fig. 3 The force of the nail and its arm to the rotation center

having each nail force and its vertical distance to the center of rotation, the moment produced by each nail force is equal to:

$$M = T_i r_i \sin(\theta_i - \alpha) \quad (19)$$

where T_i is the nails force, r_i is the length of the line extended from the center of rotation (point O) to the intersection point of each nail and the failure surface, θ_i is the angle between the line r_i and the horizontal direction, and α is the angle of the nails with respect to the horizontal direction. Therefore, by obtaining r_i from Eq. 2, the energy dissipation due to all nails was calculated as follows:

$$D_n = r_0 \omega \sum_{i=1}^n T_i e^{(\theta_i - \theta_0) \tan \phi} \sin(\theta_i - \alpha) \quad (20)$$

where n is the number of the nail layers at the wall height.

According to Fig. 4, the angle θ_i is a function of the vertical distance between the i th nail and the top of the wall, Z_i . Therefore:

$$Z_i = r_i \sin \theta_i - r_0 \sin \theta_0 - \overline{ef} \sin \alpha \quad (21)$$

where \overline{ef} is the nail length in the failed soil volume and can be obtained as follows:

$$\overline{ef} = \frac{r_i \cos \theta_i - r_h \cos \theta_h - (H - Z_i) \cot \beta}{\cos \alpha} \quad (22)$$

The nail force depends on the shear strength between the soil and the nail length outside the failure line, l_i , which can be calculated by subtracting Eq. 22 from the total length of each nail. Therefore, the nail force can be calculated as follows:

$$T_i = \frac{q_u \pi D_{DH} l_i}{S_H} \quad (23)$$

where q_u is the bond strength between the nails and the surrounding soil, D_{DH} is the drillhole diameter, and S_H is the horizontal spacing between the nails.

3.3.3 The Total Energy Dissipation

The total energy dissipation in the whole mechanism was obtained as follows:

$$D = D_c + D_n \quad (24)$$

3.4 The Factor of Safety

The upper bound method is based on the principle of virtual work, which states that the work of external forces applied to a failure mechanism is equal to the internal energy dissipated in the mechanism, i.e., $W = D$. The general form of the factor of safety, FS, is equal to the ratio of the resistant term, i.e., D , to the active term, i.e., W . Therefore, by

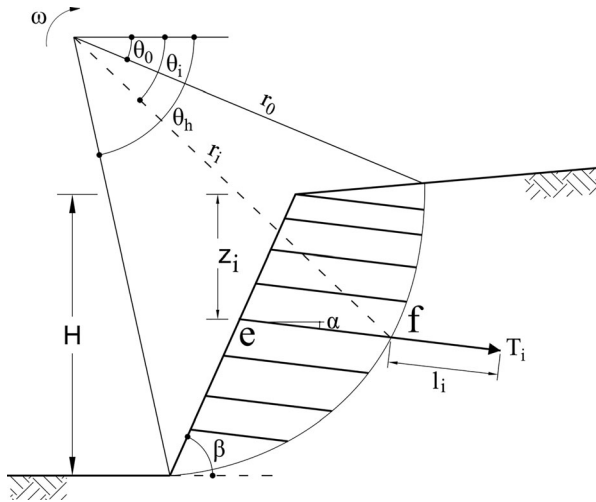


Fig. 4 The nail length outside of the failure zone

replacing the relevant equations into the general form of the equation of the factor of safety, *FS* can be obtained as follows:

$$\begin{aligned}
 FS = & \left\{ \frac{cr_0^2\omega}{2\tan\varphi} \left[e^{2(\theta_h-\theta_0)\tan\varphi} - 1 \right] + r_0\omega \sum_{i=1}^n T_i e^{(\theta_i-\theta_0)\tan\varphi} \sin(\theta_i-\alpha) \right\} / \left\{ (1-k_v)\omega\gamma r_0^3(f_1-f_2-f_3) \right. \\
 & + k_h\omega\gamma r_0^3(f_4-f_5-f_6) + \omega qL\cos\lambda(1-k_v) \left(r_0\cos\theta_0 - \frac{L}{2}\cos\lambda \right) \\
 & \left. + \omega qL\sin\lambda k_h \left(r_0\cos\theta_0 - \frac{L}{2}\cos\lambda \right) \right\} \quad (25)
 \end{aligned}$$

3.5 Optimization

The considered failure mechanism has two sets of known and unknown parameters. The known parameters include:

1. The soil parameters, including the friction angle (ϕ), cohesion (c), and the unit weight (γ).
2. The geometrical parameters of the nailed wall including the height (H), the angle of the wall to the horizontal direction (β), and the ground surface angle with respect to the horizon (λ).
3. The nail specifications including the length (L_n), the angle to the horizontal direction (α), the drillhole diameter (D_{DH}), the horizontal and vertical spacings between the nails (S_H and S_V), the bond strength (q_u), and the parameter Z_i .

The unknown parameters should be determined using an optimization technique in a way that the best (lowest) possible value of the factor of safety can be achieved. The smallest factor of safety corresponds to the best failure surface that its location depends on θ_0 , θ_i , and θ_h . As already stated, θ_0 is equal to the soil internal friction angle, which is a known parameter. Therefore, the unknowns of the problem are θ_i and θ_h , which should be optimized in order to obtain the least possible value for the safety factor. In the present study, the optimization was performed using the genetic algorithm provided

in the MATLAB program. For the optimized mechanism to be kinematically admissible, the following constraints were taken into account:

$$\theta_0 < \theta_h < \frac{\pi}{2} + \phi \quad (26)$$

$$\theta_0 < \theta_1 < \dots < \theta_h \quad (27)$$

Also, considering that the angle θ_i depends on the distance between the nail head and the ground surface (Z_i), Eq. 21 was also considered one of the constraints of the problem.

4 Verification of the Results

4.1 Static Analysis

The factor of safety obtained from the formulation developed in the present paper was compared with the results of back-predicting the full-scale test conducted on a soil nail wall in 1986 for the French national research project, Clouterre (Plumelle et al. 1990). The cross-section of this wall is shown in Fig. 5. The angle between the nails and the horizontal direction was considered to be equal to 15° , and the horizontal and vertical spacing of the nails was considered equal to 1.15 and 1 m, respectively. The first and last rows of the nails are 16 mm in diameter and 6 m in length, while the rest of the nails are 40 mm in diameter and 8 m in length. Also, the cohesion, the internal friction angle, and the unit weight of the soil behind the wall were considered equal to 3 kPa, 38° , and 20 kN/m^3 , respectively.

Stability analysis of this wall in the static condition was performed using the Morgenstern–Price limit equilibrium method, which resulted in a factor of safety equal to 1.413 (Plumelle et al. 1990). The upper bound formulation presented in the current paper was also used for obtaining the safety factor, which resulted in $FS = 1.418$. Therefore, these two methods have good consistency with each other.

4.2 Seismic Analysis

Ghosh and Paul (Ghosh and Paul 2016) considered seismic analysis of soil nail walls under horizontal earthquake load. The specification of their models is $H = 10 \text{ m}$, $\lambda = 0^\circ$,

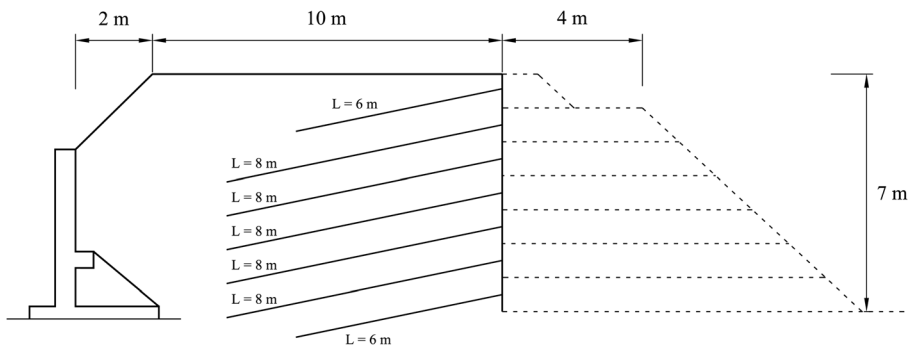


Fig. 5 Cross-section of the soil nail wall in the Clouterre project (Plumelle et al. 1990)

$q = 50$ kPa, $L_n = 7$ m, $S_H = S_V = 70$ cm, $c = 5$ kPa, and $k_v = 0$. Considering different values of the soil friction angle and various amounts of the horizontal earthquake accelerations, Table 1 presents the safety factor obtained by Ghosh and Paul (Ghosh and Paul 2016) and the method presented in the current paper. Good conformity between the results of these two methods can be seen.

5 Sensitivity Analyses

To investigate the effect of different parameters on the safety factor of soil nail walls, a general sketch of the soil nail wall, as shown in Fig. 6, was considered. Three different magnitudes of H , including 5 m, 10 m, and 15 m, were taken into account. Extensive sensitivity analyses were performed, considering the parameters presented in Table 2. For investigating the effect of each parameter on the safety factor, a wide range was considered for most of the parameters, while a constant magnitude was considered for the rest of the parameters.

5.1 The Effect of Soil Internal Friction Angle

Figure 7 shows the variation of FS versus ϕ . As can be seen, FS increases by increasing the internal friction angle. Also, the rate of increment of the FS was increased for large values of ϕ . Increasing the horizontal acceleration of the earthquake (k_h) and increasing the trench height (H) also decrease the safety factor.

5.2 The Effect of Soil Cohesion

Figure 8 shows the variation of FS versus c . By increasing the cohesion from 5 to 45 kPa, the maximum increase in FS is equal to 22%, 19%, and 18% for the walls with $H = 5$ m, 10 m, and 15 m, respectively. Therefore, it can be concluded that increasing the height of the wall results in reducing the effect of cohesion on the safety factor. For each magnitude of c , increasing the earthquake horizontal acceleration results in reducing the safety factor.

5.3 The Effect of Surcharge

Given that many excavations are carried out next to the buildings or any other construction activities, it is essential to investigate the effect of surcharge loads on

Table 1 Comparison between the FS obtained from the present study and Ghosh and Paul (Ghosh and Paul 2016) method

ϕ°	30°			35°			40°		
FS k_h	0	0.1	0.2	0	0.1	0.2	0	0.1	0.2
Present study	1.412	1.083	0.862	2.00	1.47	1.18	2.86	1.94	1.58
Ghosh and Paul (Ghosh and Paul 2016)	1.405	1.072	0.839	1.99	1.48	1.16	2.85	1.93	1.46
Difference (%)	0.71	0.93	3.60	0.50	0.68	1.72	0.35	0.52	8.22

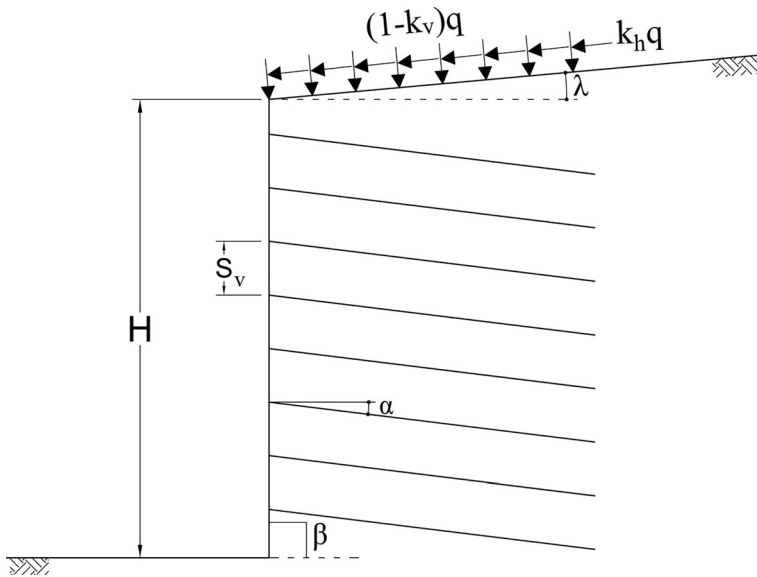


Fig. 6 Examined model of the nailing trench

the safety factor of the nailed wall. Figure 9 shows the variation of FS versus q . According to the results, for all considered values of k_h , increasing the surcharge results in decreasing the safety factor. As the surcharge increases, the rate of reduction of the safety factor decreases.

5.4 The Effect of Ground Surface Inclination

Figure 10 shows the variation of FS versus λ . The safety factor decreases with increasing the inclination of the ground surface. By increasing λ from zero to 35° , a maximum of 31%, 54%, and 29% reduction of the safety factor was observed for the walls with $H = 5$ m, 10 m, and 15 m, respectively.

Table 2 The parameters considered in the sensitivity analyses

Parameter	Range	Value
γ (kN/m ³)	-	19
ϕ°	15–40	32
c (kPa)	12–45	12
q (kN/m)	0–60	20
λ°	0–35	0
S_H and S_V (m)	1–2	1.5
D (mm)	0–20	10
α°	-	15
β°	-	90
q_u (kPa) (Lazarte et al. 2003)	-	100

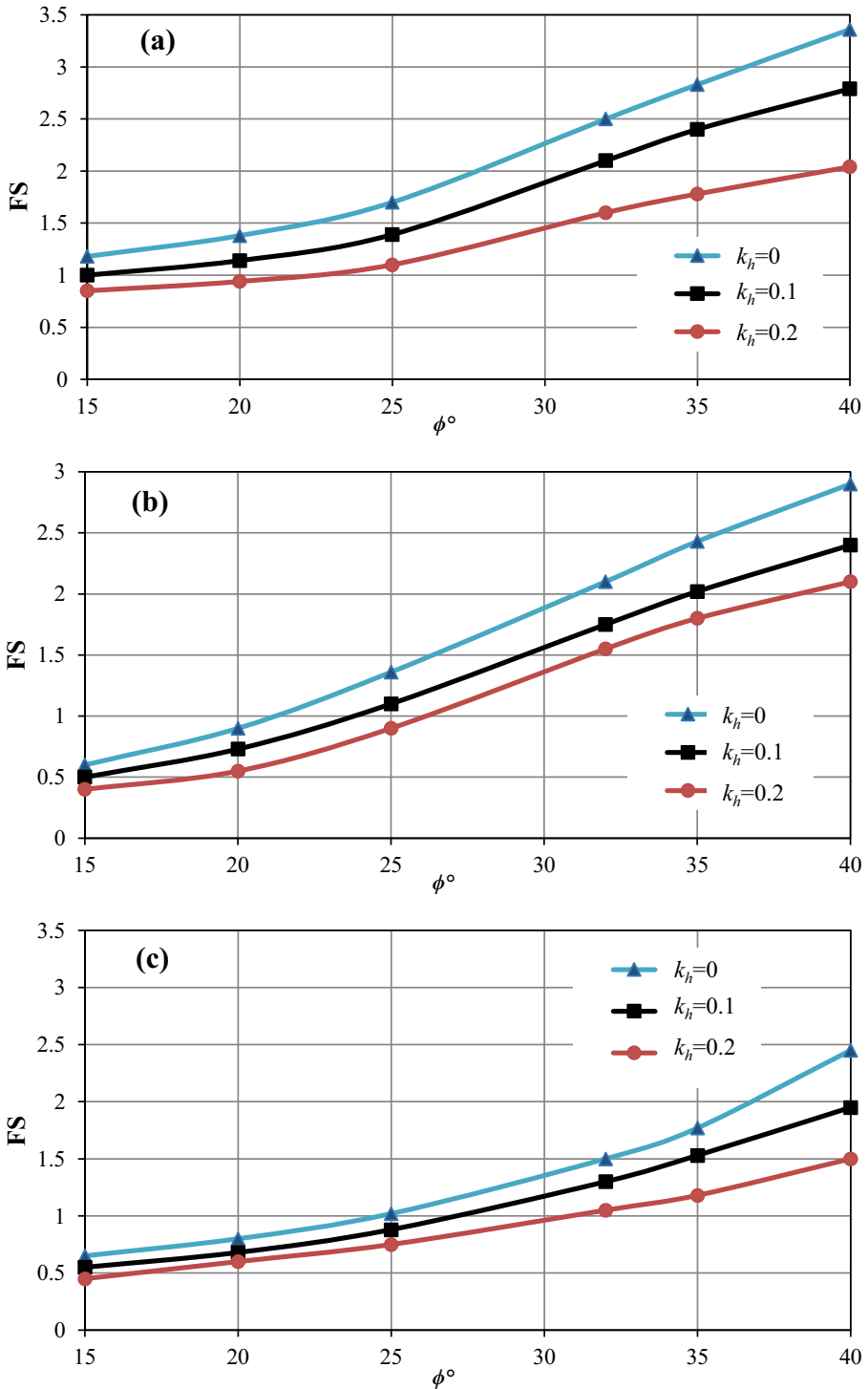


Fig. 7 Variation of FS versus ϕ , considering a $H=5$ m, b $H=10$ m, and c $H=15$ m

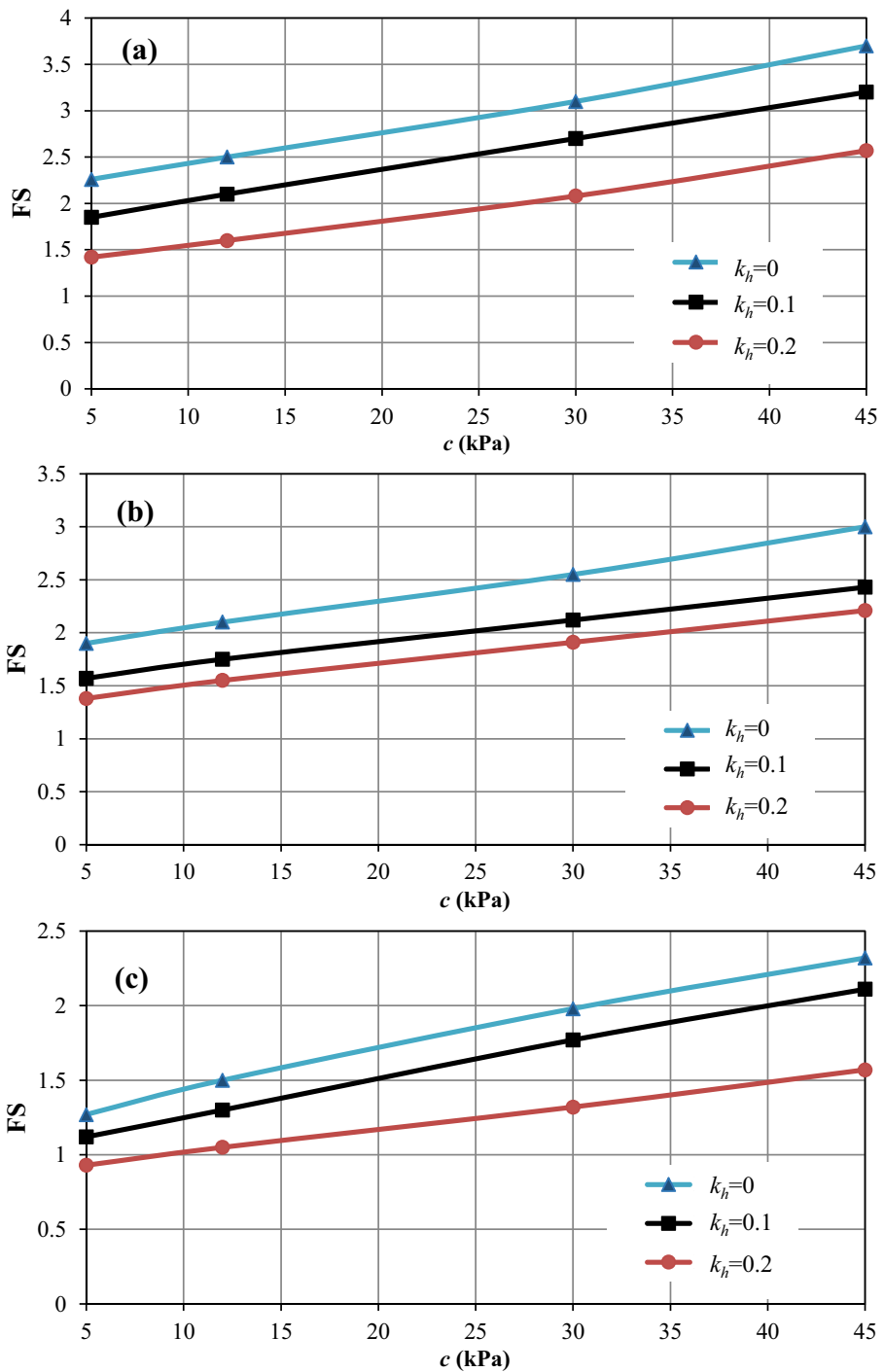


Fig. 8 Variation of FS versus c , considering **a** $H=5$ m, **b** $H=10$ m, and **c** $H=15$ m

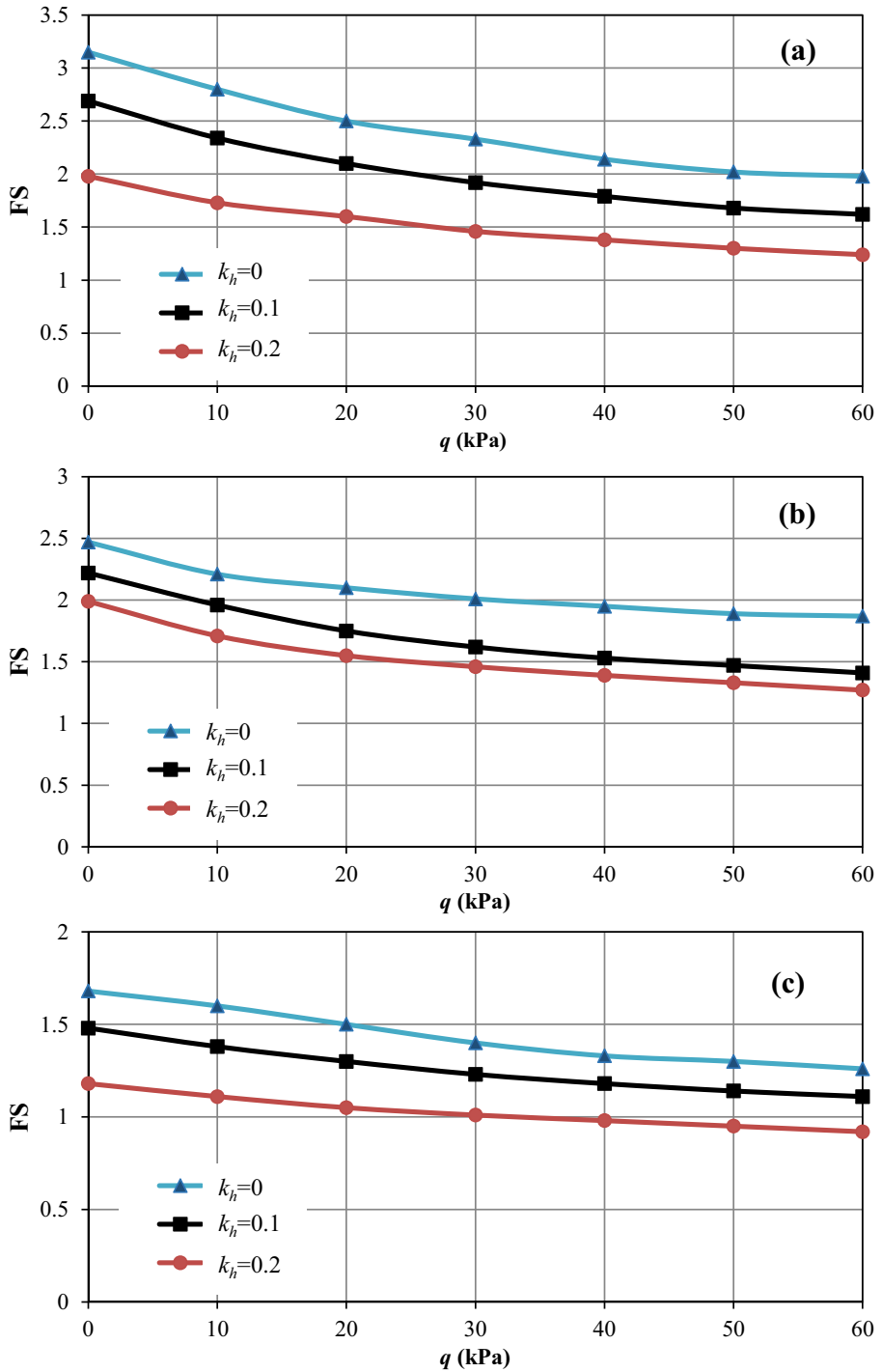


Fig. 9 Variation of FS versus q , considering a $H = 5$ m, b $H = 10$ m, and c $H = 15$ m

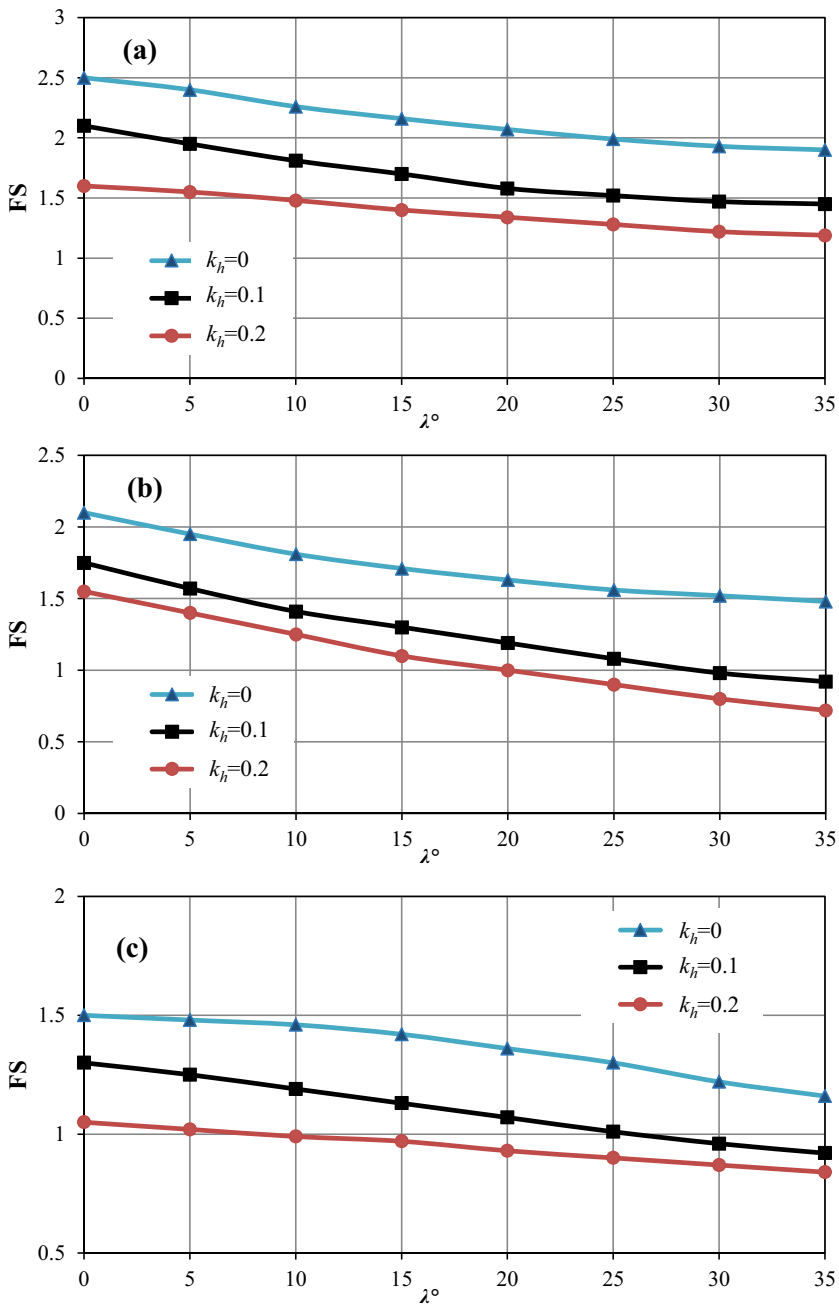


Fig. 10 Variation of FS versus λ , considering **a** $H=5$ m, **b** $H=10$ m, and **c** $H=15$ m

5.5 The Effect of Nail Length

Figure 11 shows the variation of FS versus L_n . The results show that the length of the nails has a considerable effect on the safety factor. In the case of $H=$

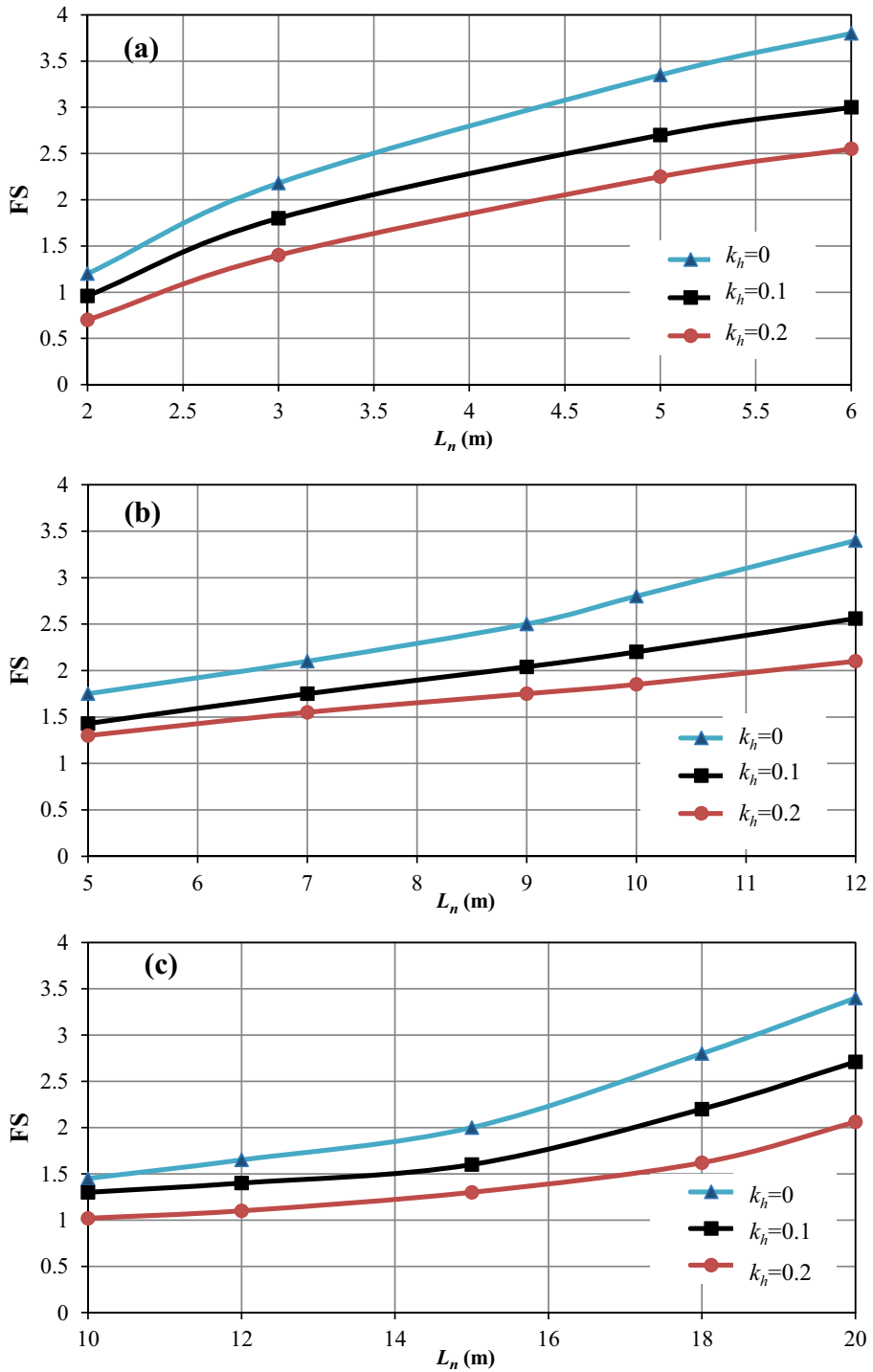


Fig. 11 Variation of FS versus L_n , considering a $H = 5$ m, b $H = 10$ m, and c $H = 15$ m

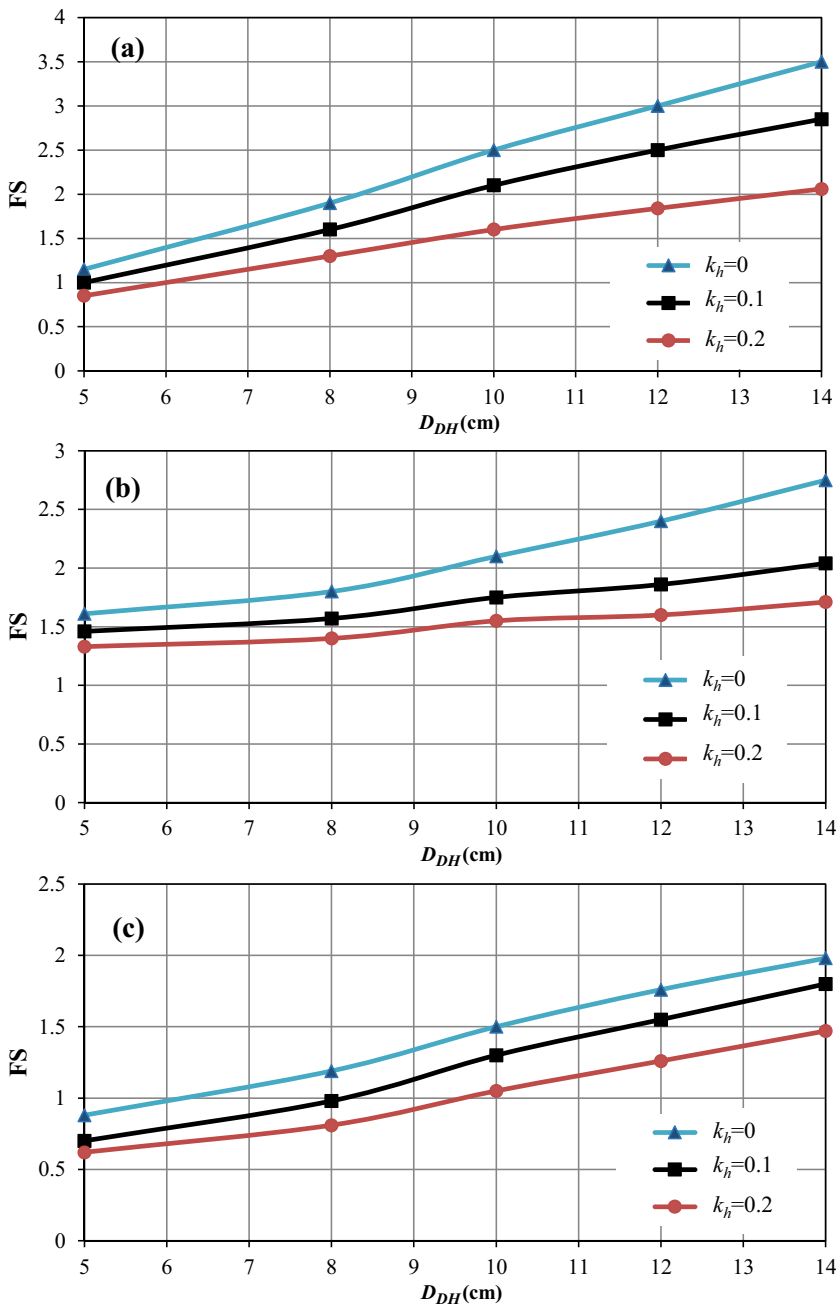


Fig. 12 Variation of FS versus D_{DH} , considering a $H=5$ m, b $H=10$ m, and c $H=15$ m

5 m, the safety factor of the case with $L_n=6$ m is 2.64 times the case with $L_n=2$ m. Also, for the case of $H=10$ m, by increasing the nail length from 5 to 12 m, the maximum increase in the safety factor is about 94%. For a 15 m

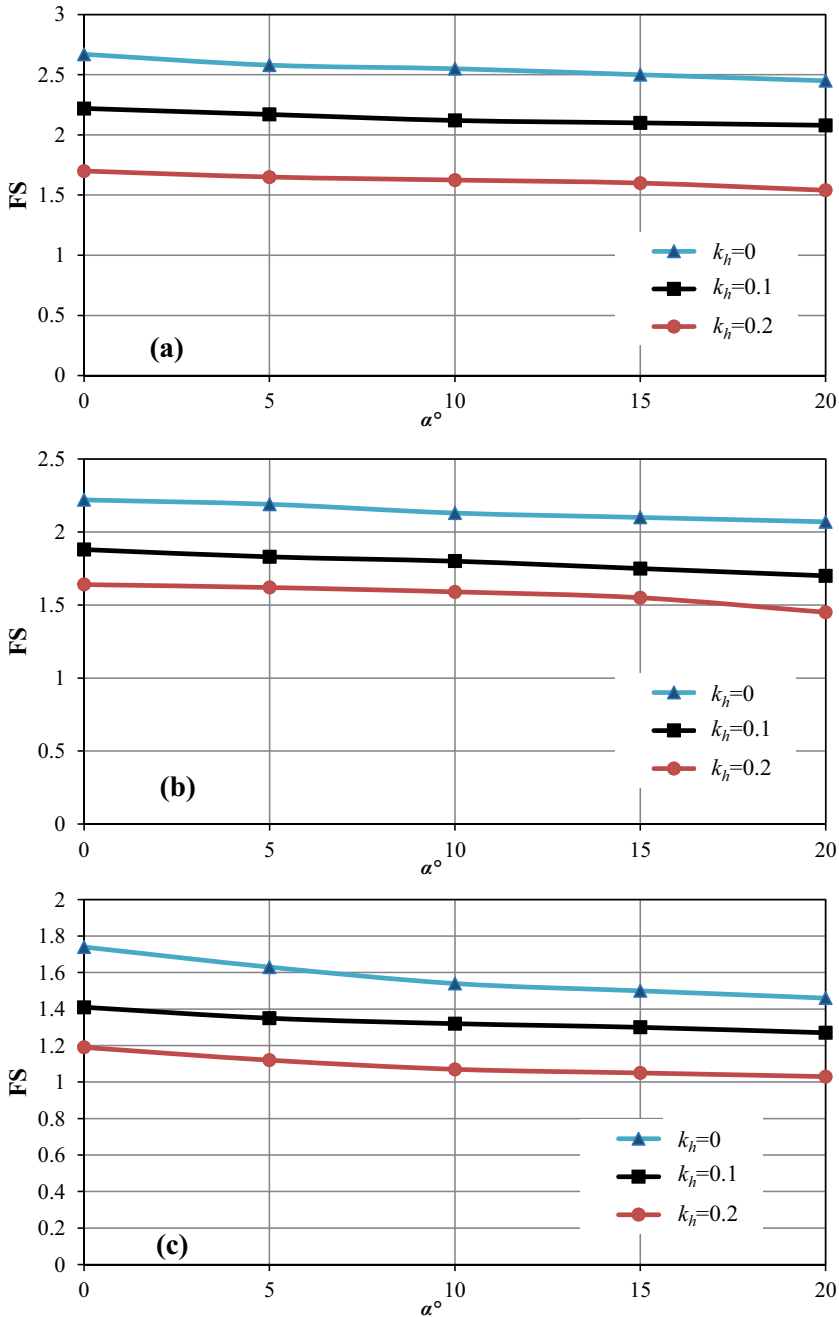


Fig. 13 Variation of FS versus α , considering **a** $H = 5$ m, **b** $H = 10$ m, and **c** $H = 15$ m

tall wall, by increasing the nail length from 10 to 20 m, the maximum increase in the safety factor is about 134%.

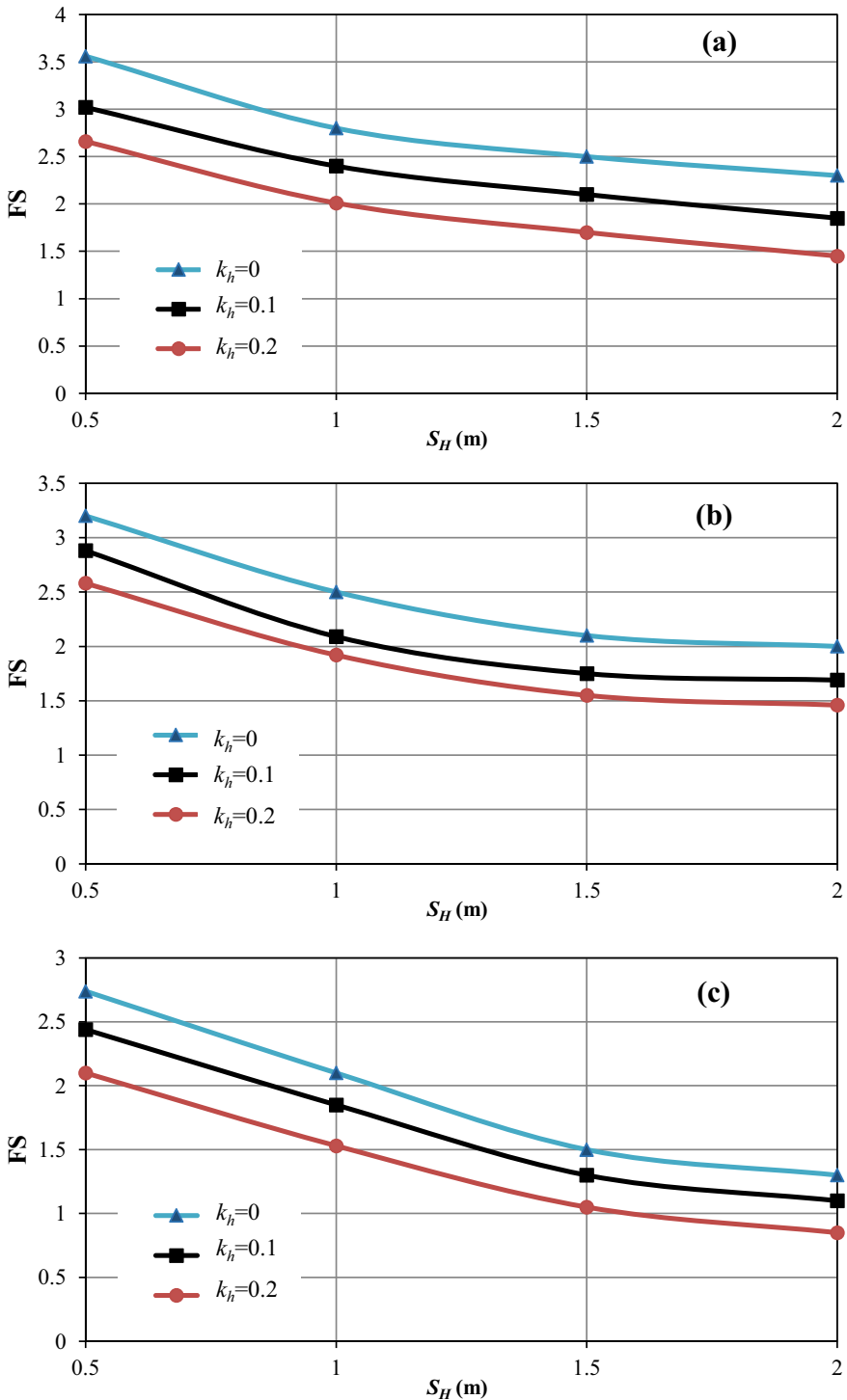


Fig. 14 Variation of FS versus S_H , considering a $H = 5$ m, b $H = 10$ m, and c $H = 15$ m

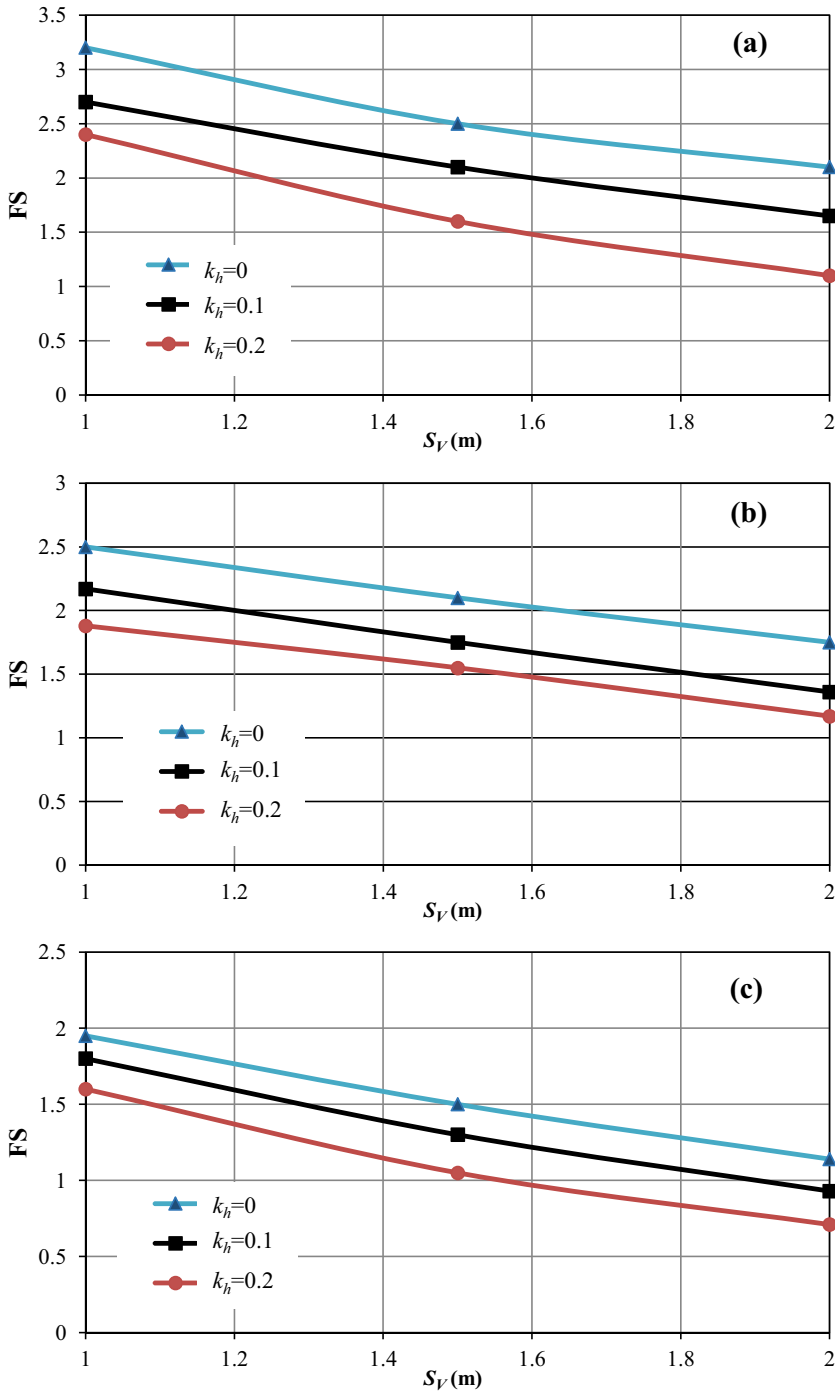


Fig. 15 Variation of FS versus S_V , considering a $H = 5$ m, b $H = 10$ m, and c $H = 15$ m

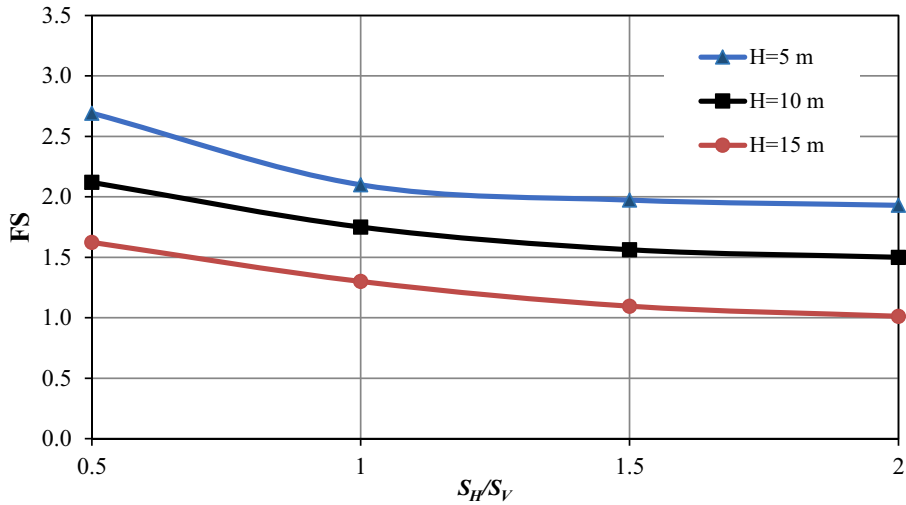


Fig. 16 Variation of FS versus S_H/S_V ratio

5.6 The Effect of Drillhole Diameter

Figure 12 shows the variation of FS versus D_{DH} . As can be seen, for all considered values of k_h , increasing the drillhole diameter has a significant effect on the safety factor, which is due to the increase in the resistance force produced by the bond strength. In the 5 m, 10 m, and 15 m tall walls, by increasing the drillhole diameter from 5 to 14 cm, the maximum increase in the safety factor is approximately equal to 204%, 71%, and 157%, respectively.

5.7 The Effect of Nail Inclination

Figure 13 shows the variation of FS versus α . It is clear that for all considered values of k_h , the inclination of the nails to the horizontal direction has a small effect on the factor of safety. For the walls with $H=5$ m, 10 m, and 15 m, the maximum reduction of the FS is equal to 9%, 12%, and 16%, respectively.

5.8 The Effect of Nail Horizontal Spacing

Figure 14 shows the effect of nail horizontal spacing on FS. As can be seen, by increasing the S_H , the safety factor decreases. For the S_H values approximately smaller than 1.5 m, the rate of reduction is more sensible than the rate of reduction of FS in the case of $S_H > 1.5$ m. For the walls with $H=5$ m, 10 m, and 15 m, by increasing S_H from 0.5 to 2 m, the FS decreased about 45%, 43%, and 60%, respectively.

5.9 The Effect of Nail Vertical Spacing

Figure 15 illustrates the variation of FS with S_V . For all considered values of k_h , FS decreases with increasing S_V with an approximately linear rate. By increasing the nail

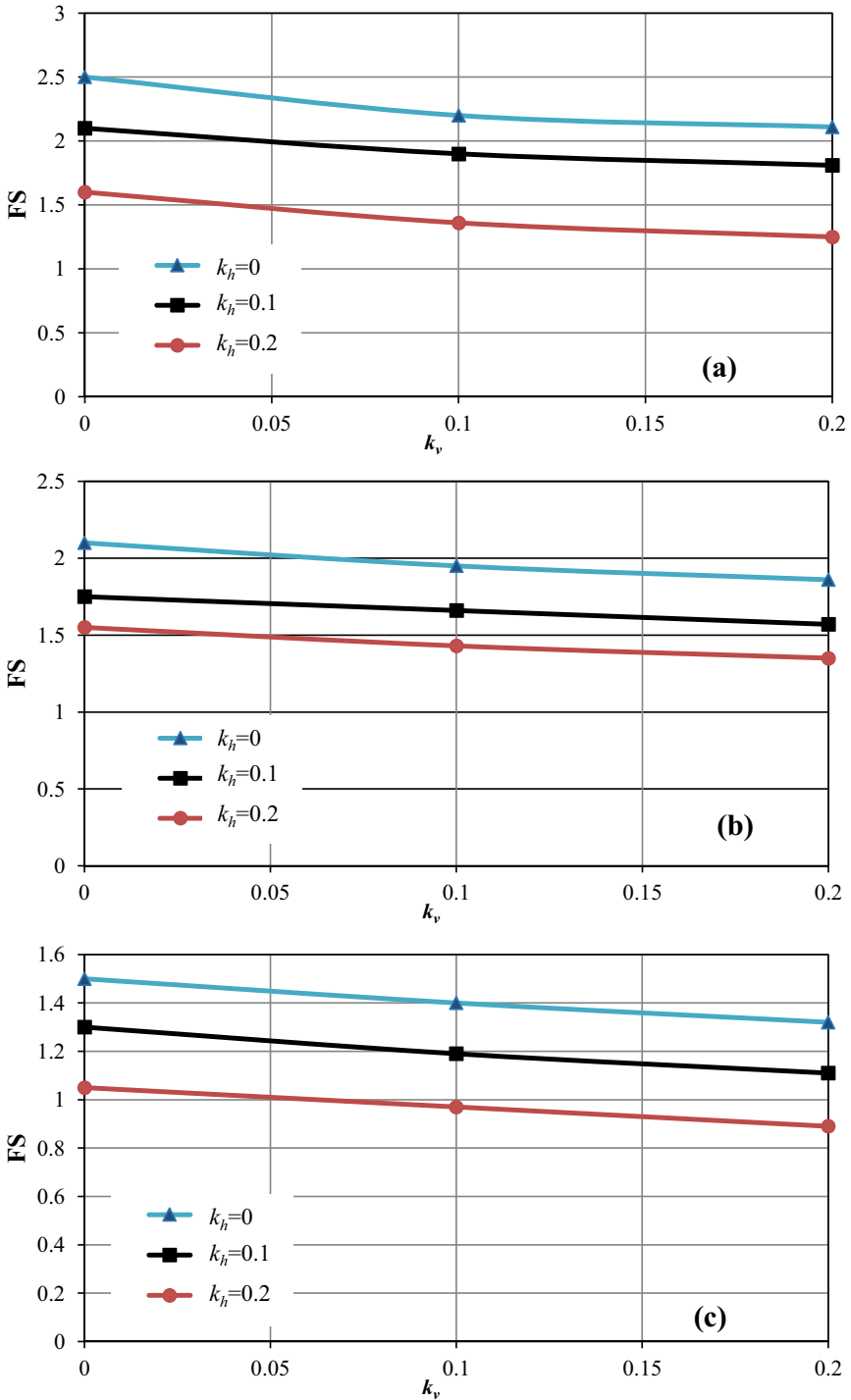


Fig. 17 Variation of FS versus k_v , considering **a** $H = 5$ m, **b** $H = 10$ m, and **c** $H = 15$ m

vertical spacing from 1 to 2 m, the safety factor decreased about 54%, 38%, and 56% for the wall heights equal to $H = 5$ m, 10 m, and 15 m, respectively.

5.10 The Effect of Nail Horizontal to Vertical Spacing Ratio

Assuming $k_h = 0.1$, Fig. 16 illustrates the variation of FS with S_H/S_V ratio. It is clear that increasing the S_H/S_V ratio results in decreasing FS, but the rate of this reduction decreases with increasing the S_H/S_V ratio. For S_H/S_V smaller than 1.5, the rate of reduction of FS is more sensible than the cases of $S_H/S_V > 1.5$. For the walls with $H = 5$ m, 10 m, and 15 m, increasing S_H/S_V from 0.5 to 2 results in decreasing FS about 28%, 30%, and 37%, respectively.

5.11 The Effect of Earthquake Vertical Acceleration

The effect of earthquake vertical acceleration (k_v) on the stability of soil nail walls was not investigated sufficiently by previous researchers. The upper bound formulation proposed in the present study has the capability of considering the earthquake vertical acceleration. As shown in Fig. 17, increasing k_v results in decreasing FS, but its effect is less than the effect of the horizontal earthquake acceleration. In the walls with $H = 5$ m, 10 m, and 15 m, increasing k_v from zero to 0.2 leads to decreasing the safety factor by 22%, 13%, and 15%, respectively.

6 Conclusions

The safety factor of soil nail walls subjected to static and seismic loadings was studied. The main conclusions of the present paper are as follows:

- Increasing the parameters like the soil cohesion, internal friction angle, the nail length, and the drillhole diameter results in increasing the factor of safety.
- Increasing the parameters like the surcharge, the inclination of the nails and the ground surface, and the horizontal and vertical spacings of the nails results in decreasing the factor of safety.
- Increasing the horizontal and vertical accelerations of earthquake results in decreasing the factor of safety.
- The obtained results show that the effect of the horizontal acceleration of the earthquake on reducing the factor of safety is more paramount than the effect of the vertical acceleration of the earthquake.

Code Availability Some or all parts of the code that supports the findings of this study are available from the corresponding author upon reasonable request.

Data Availability Some or all data and material that support the findings of this study are available from the corresponding author upon reasonable request.

Compliance with ethical standards

Conflict of Interest The authors declare that they have no conflict of interest.

References

- Babu, G.L.S., Rao, R.S., Dasaka, S.M.: Stabilisation of vertical cut supporting a retaining wall using soil nailing: a case study. *Ground Imp.* **11**, 157–162 (2007)
- Chen W.F., Liu X.L.: *Limit analysis in soil mechanics*. Elsevier Science, Netherlands (1990)
- Clarke, S.D., Gilbert, M., Smith, C.C.: Modelling discrete soil reinforcement in numerical limit analysis. *Can. Geotech. J.* **50**(7), 705–715 (2013)
- Lazarte, C.A., Elias, V., Espinoza, D., Sabatini, P.J.: *Geotechnical Engineering Circular No. 7: Soil nail walls*. U.S. Department of Transportation, Washington, D.C. (2003)
- Ghosh, S., Paul, A.: Analysis of soil nail excavation considering Rayleigh wave with log-spiral failure surface. *Int. J. Geosynth. Ground Eng.* **2**(18), 1–11 (2016)
- Giri, D., Sengupta, A.: A kinematic limit approach for the stability analysis of nailed soil slopes. *Asian J. Civ. Eng. (building & housing)*. **10**(2), 163–176 (2009)
- Giri, D., Sengupta, A.: Dynamic behavior of small-scale model of nailed steep slope. *Geomech. Geoeng.* **5**(2), 99–108 (2010)
- He, S., Ouyang, C., Luo, Y.: Seismic stability analysis of soil nail reinforced slope using kinematic approach of limit analysis. *Environ. Earth Sci.* **66**, 319–326 (2012)
- Jaya, V., Joy, A.: An investigation on the dynamic behaviour of soil nail walls. *J. Civ. Eng. Sci.* **2**(4), 241–249 (2013)
- Meenal, G., Saran, S., Mittal, S.: Pseudo-static analysis of soil nailed excavations. *Geotech. Geol. Eng.* **27**, 571–583 (2009)
- Michalowski, R.L.: Limit analysis in stability calculations of reinforced soil structures. *Geotext. Geomembr.* **16**, 311–331 (1998)
- Mittal, S.: Soil nailing application in erosion control an experimental study. *Geotech. Geol. Eng.* **24**, 675–688 (2006)
- Moradi, M., Pooresmaeili Babaki, A., Sabermahani, M.: Effect of nail arrangement on the behavior of convex corner soil-nailed walls. *J. Geotech. Geoenviron. Eng.* **146**(5), 04020026:1–12 (2020)
- Plumelle, C., Schlosser, F., Delage, P., Knochenmus, G.: French national research project on soil nailing: CLOUTERRE. *Geotechnical Special Publication No. 25*, pp. 660–675. ASCE, New York (1990)
- Rawat, S., Zodinpuui, R., Manna, B., Sharma, K.G.: Investigation on failure mechanism of nailed soil slopes under surcharge loading: testing and analysis. *Geomech. Geoeng.* **9**(1), 18–35 (2013)
- Sharma, M., Choudhury, D., Samanta, M., Sarkar, S., Annareddy, V.S.R.: Analysis of helical soil-nailed walls under static and seismic conditions. *Can. Geotech. J.*, **57**(6), 785–800 (2020)
- Yang, T., Zou, J.F., Pan, Q.J.: Three-dimensional seismic stability of slopes reinforced by soil nails. *Comput. Geotech.* **127**, 103768 (2020)
- Zhou, W.H., Yin, J.H.: A simple mathematical model for soil nail and soil interaction analysis. *Comput. Geotech.* **35**, 479–488 (2008)
- Zhou, Y.D., Cheuk, C.Y., Tham, L.G.: Numerical modeling of soil nails in loose fill slope under surcharge loading. *Comput. Geotech.* **36**, 837–850 (2009)

Publisher's Note Springer Nature remains neutral with regard to jurisdictional claims in published maps and institutional affiliations.